OPTIMUM AMBIGUITY-FREE ISOTROPIC ANTENNA ARRAYS

Houcem Gazzah†

Karim Abed-Meraim†,‡

† University of Sharjah
ECE Department. P.O. Box 27272. UAE
hgazzah@sharjah.ac.ae

‡TELECOM ParisTech
TSI Dept. Rue Dareau 75014, Paris, France
kmeriam@sharjah.ac.ae

ABSTRACT

Based on the CRB of the 2D-DOA estimation problem, we prove a condition on the sensor coordinates of a planar array to be ambiguity-free and isotropic. A systematic search of such antenna arrays is conducted leading to the identification of all possible ambiguity-free isotropic arrays. In particular, we select the arrays that outperform the popular Uniform Circular Array (UCA). It is shown that these arrays allow to enhance the DOA estimation by as much as 25%, in comparison with UCA. As the number of sensors increases, the best isotropic array tends towards the non-intuitive V-shape.

***Index Terms*—** Direction of arrival estimation

1. INTRODUCTION

This paper deals with the direction finding problem, where data collected by a set (array) of sensors is used to infer about the direction of arrival (DOA) of the emitting narrow-band source [1]. A central result in DOA estimation is the Cramer-Rao Bound (CRB) that expresses the minimum achievable mean square error (MMSE) on the azimuth and elevation angles. The matrix-valued CRB was originally proposed in the form of a sophisticated expression [2, 3] before being greatly simplified in [4]. There, it was shown to be merely a cosine function, leading to a rich interpretation about the impact of the sensor positions on the array performance.

These results lack relevance in practice, as they do not take into account the array ambiguity problem. The so-called (first-order) ambiguity occurs when steering vectors relative to two different DOAs are co-linear. A sufficient condition to ensure ambiguity-free arrays is to keep each sensor at most half-a-wavelength distant from its nearest neighbors [5].

The challenge, dealt with here, is how to incorporate this condition into the CRB. We do so by imagining that the sensors are placed along a curve in the plane at a regular spacing (equal to half the wavelength). This configuration is not restrictive at all, and supports practically all known array configurations, including the Uniform Linear Array (ULA), the Uniform Circular Array (UCA), grid arrays, etc.

The CRB from [4] serves as the starting point. Thanks to the above modeling, it is now a function of bounded (angular) parameters, and so, lends itself easily to numerical computation and optimization. In particular, isotropy is met if these parameters are the zeros of a multi-dimensional complex-valued function. We manage to simplify this condition, hence reducing the computation burden of the exhaustive search of (all possible) isotropic arrays. We target, in particular, isotropic arrays that outperform the UCA, the default choice for isotropic arrays. These show to have geometries that are not intuitive to guess otherwise, while, at the same time, offer a significant (DOA estimation) gain compared to the UCA.

The paper is organized as follows. Results on the CRB [4] are recalled in Sec. 2, then updated in Sec. 3 to include ambiguity constraints. In Sec. 4, a condition on the sensors is derived, then simplified, that characterizes isotropic ambiguity-free arrays. Based on this condition, a systematic search is conducted, and results are presented in Sec. 5, with particular attention to better-than-UCA array geometries.

2. DATA MODEL AND PREVIOUS RESULTS

A planar antenna array is made of M identical and omni-directional sensors in the (x, y) plane. The position of the m-th sensor is given by its polar coordinates ρ_m and ϕ_m to which we associate the complex number $\gamma_m \hat{=} \rho_m e^{j\phi_m}$. A source located in the far-field is characterized by its DOA angles: the azimuth Φ and the elevation Θ as depicted in Fig. 1. When the source emits a narrow-band signal centered at frequency c/λ, the M-dimensional output of the antenna array can be expressed as phased replicas of the emitted signal, as follows

$$\begin{aligned}\mathbf{x}(t) &\hat{=} [x_1(t)\cdots x_M(t)]^T \\ &= \begin{bmatrix} \exp\left(2j\pi\frac{\rho_1}{\lambda}\sin(\Theta)\cos(\Phi-\phi_1)\right) \\ \vdots \\ \exp\left(2j\pi\frac{\rho_M}{\lambda}\sin(\Theta)\cos(\Phi-\phi_M)\right)\end{bmatrix} s(t)+\mathbf{n}(t) \\ &\hat{=} \mathbf{a}(\Phi,\Theta)s(t)+\mathbf{n}(t),\end{aligned}$$

where the m-th entry of $\mathbf{x}(t)$ [resp. $\mathbf{n}(t)$] is the signal (resp. noise) component collected at sensor m at time index t. They are assumed to be Gaussian-distributed, zero-mean, mutually-independent and spatially and temporally white, with respective variances σ_s^2 and σ_n^2.

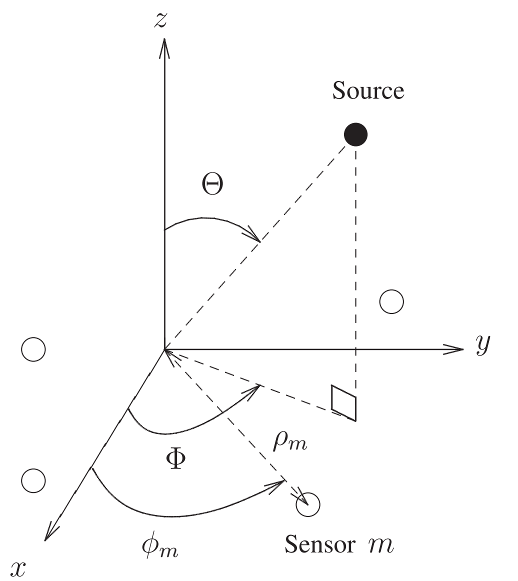

Fig. 1. Planar array and source DOAs.

In the single source case with N signal snapshots, the lowest possible estimation error is expressed by the CRB [4]

$$\mathbf{C} \hat{=} \begin{bmatrix} \mathbf{C}_{\Phi\Phi} & \mathbf{C}_{\Phi\Theta} \\ \mathbf{C}_{\Theta\Phi} & \mathbf{C}_{\Theta\Theta} \end{bmatrix}$$

where

$$\begin{aligned}
\mathbf{C}_{\Phi\Phi} &= \frac{C_{\mathrm{SNR}}}{N} \frac{1}{\sin^2(\Theta)} \mathcal{C}(\Phi) \\
\mathbf{C}_{\Theta\Theta} &= \frac{C_{\mathrm{SNR}}}{N} \frac{1}{\cos^2(\Theta)} \mathcal{C}\left(\Phi + \frac{\pi}{2}\right) \\
\mathbf{C}_{\Phi\Theta} &= -\frac{C_{\mathrm{SNR}}}{N} \frac{1}{\sin(2\Theta)} \frac{\Im\left[T_2 \exp(-2j\Phi)\right]}{T_0^2 - |T_2|^2}
\end{aligned}$$

with $C_{\mathrm{SNR}} \hat{=} (\sigma_n^2/\sigma_s^2)\left[1 + \sigma_n^2/(M\sigma_s^2)\right]/(4\pi^2)$ and

$$\mathcal{C}(\Phi) \hat{=} \frac{T_0 + \Re\left[T_2 \exp(-2j\Phi)\right]}{T_0^2 - |T_2|^2},$$

$\Re(x)$ and $\Im(x)$ being the real and imaginary parts of x, respectively. The function $\mathcal{C}(\Phi)$ depends only on the source azimuth angle and on the geometrical parameters

$$\begin{aligned}
T_0 &\hat{=} \sum_{m=1}^{M} |\gamma_m|^2 - \frac{1}{M}\left|\sum_{m=1}^{M} \gamma_m\right|^2 \\
T_2 &\hat{=} \sum_{m=1}^{M} \gamma_m^2 - \frac{1}{M}\left(\sum_{m=1}^{M} \gamma_m\right)^2 .
\end{aligned} \tag{1}$$

The latter, when equal to zero, indicates that the considered array is isotropic because, then, $\mathcal{C}(\Phi)$ is a constant (DOA-independent), and so are all the entries of the CRB matrix.

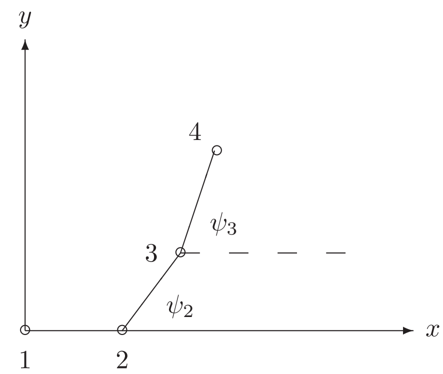

Fig. 2. Sensor numbering and parameters ψ_k.

3. AMBIGUITY-FREE ANTENNA ARRAYS

Without loss of generality, we place the first sensor at the origin, the second sensor on the $x > 0$ axis and the third sensor in the $y \geq 0$ semi-plane. Hence, $\gamma_1 = 0$, $\gamma_2 = d$ and $\Im(\gamma_3) > 0$.

Now, to ensure a maximum inter-sensor spacing d (typically chosen to be equal to half a wavelength), we imagine that the sensors are uniformly placed along a curve in the (x, y) plane, or equivalently, that a curve can be drawn that joins the uniformly spaced sensors, numbered 1 (placed at the origin), 2, $\cdots$, M. Two consecutive sensors would, hence, verify $|\gamma_k - \gamma_{k-1}| = d$ or also

$$\gamma_k = \gamma_{k-1} + d\exp(j\psi_{k-1})$$

for some angle $\psi_{k-1} \in [-\pi, \pi[$, for all $k \geq 2$. The array geometry is entirely characterized by parameters $\gamma_3, \cdots, \gamma_M$, or equivalently by angles $\psi_2, \cdots, \psi_{M-1}$, where $\psi_2 \in [0, \pi[$ and $\psi_k \in [-\pi, \pi[$ for $k > 2$, ψ_1 being equal to zero. For $k \geq 2$, we can write $\gamma_{k+1}/d = 1 + \sum_{l=2}^{k} \exp(j\psi_l)$ so that

$$\begin{aligned}
\frac{\sum_{m=3}^{M} \gamma_m}{d} &= M - 2 + \sum_{m=2}^{M-1} (M-m)\exp(j\psi_m) \\
\frac{\sum_{m=3}^{M} \gamma_m^2}{d^2} &= M - 2 + 2\sum_{m=2}^{M-1} (M-m)\exp(j\psi_m) \\
&\quad + \sum_{m=3}^{M} \left[\sum_{l=2}^{m-1} \exp(j\psi_l)\right]^2 .
\end{aligned}$$

After tedious manipulations, we obtain

$$\begin{aligned}
M\frac{T_2}{d^2} &= M - 1 + 2\sum_{m=2}^{M-1} (M-m)e^{j\psi_m} \\
&- \left[\sum_{m=2}^{M-1} (M-m)e^{j\psi_m}\right]^2 + M\sum_{m=2}^{M-1}\left[\sum_{l=2}^{m} e^{j\psi_l}\right]^2
\end{aligned} \tag{2}$$

4. AMBIGUITY-FREE ISOTROPIC ANTENNA ARRAYS

Eqt. (2) shows how the set of parameters $\psi_2, \cdots, \psi_{M-1}$ affect the directivity of the antenna array. Of interest, here, are situations where T_2 is zero, characterizing isotropic arrays.

Such isotropic arrays can be identified by evaluating the scalar function in (2) for all possible values of the $M-2$ parameters $\psi_2, \cdots, \psi_{M-1}$ and check when this happens to be (close to) zero. To reduce the complexity of such a systematic search, we notice that the expression in (2) is a second order polynomial in $\exp(j\psi_{M-1})$. In fact, by denoting

$$\begin{aligned}
U_0 &\hat{=} \sum_{m=2}^{M-2} \exp(j\psi_m) \\
U_1 &\hat{=} 1 + \sum_{m=2}^{M-2} m \exp(j\psi_m) \\
U_2 &\hat{=} 1 + \sum_{m=2}^{M-2} \left[\sum_{l=2}^{m} \exp(j\psi_l) \right]^2,
\end{aligned}$$

we ultimately prove that

$$M\frac{T_2}{d^2} = (M-1)\exp(2j\psi_{M-1}) + 2U_1 \exp(j\psi_{M-1}) + C \quad (3)$$

where

$$C \hat{=} M + 2MU_0U_1 + (M - M^2)U_0^2 + M(U_2 - 1) - U_1^2$$

For the array to be isotropic, $\exp(j\psi_{M-1})$ needs to be a zero of the second order polynomial in the RHS of (3). Therefore, it must verify

$$\exp(j\psi_{M-1}) = \frac{-U_1 \pm \left[U_1^2 + (1-M)C\right]^{1/2}}{M-1}$$

where $U_1^2 + (1-M)C$ can be proved to be equal to $M\left\{[U_1 + (1-M)U_0]^2 + (1-M)U_2\right\}$.

Finally, an array characterized by $\psi_2, \cdots, \psi_{M-1}$ is isotropic iff $\psi_2, \cdots, \psi_{M-2}$ verify either $U_1 + \sqrt{M}\left\{[U_1 + (1-M)U_0]^2 + (1-M)U_2\right\}^{1/2}$ or $U_1 - \sqrt{M}\left\{[U_1 + (1-M)U_0]^2 + (1-M)U_2\right\}^{1/2}$ has a modulus equal to $M-1$. Then, ψ_{M-1} is given by the argument of the one among

$$\frac{U_1 \pm \sqrt{M}\left\{[U_1 + (1-M)U_0]^2 + (1-M)U_2\right\}^{1/2}}{1-M} \quad (4)$$

that happens to have a modulus equal to 1.

Finding $\psi_2, \cdots, \psi_{M-1}$ satisfying (2) is zero simplifies to finding $\psi_2, \cdots, \psi_{M-2}$ satisfying (4) has a modulus one, reducing by one the dimension of the search space. In practice, the number of sensors is limited, while, the grid resolution is high. Consequently, this simplification significantly reduces the complexity of the greedy search (by 360, for example, if tested values of ψ_m are taken at a 1° interval). This taken into consideration, complexity is not a critical issue, since we are dealing, here, with an off-line optimization problem.

5. RESULTS OF THE SYSTEMATIC SEARCH

A greedy search is conducted over the $(M-3)$-dimensional space to determine parameters $\psi_2, \cdots, \psi_{M-2}$, characterizing the positions of sensors 3 to $M-1$ of an isotropic antenna array. The positions of sensor 1 and 2 are fixed while that of sensor M is completely determined by those of the remaining sensors. Parameter ψ_2 is restricted to $[0, \pi[$, while each of $\psi_3, \cdots, \psi_{M-2}$ spans $[-\pi, \pi[$.

First, we evaluate two positive scalar functions

$$\begin{aligned}
F_1(\psi_2, \cdots, \psi_{M-2}) &= |1 - |f_1(\psi_2, \cdots, \psi_{M-2})|| \\
F_2(\psi_2, \cdots, \psi_{M-2}) &= |1 - |f_2(\psi_2, \cdots, \psi_{M-2})||
\end{aligned}$$

where $f_1(\psi_2, \cdots, \psi_{M-2})$ and $f_2(\psi_2, \cdots, \psi_{M-2})$ are defined, respectively, as

$$\frac{U_1 + \sqrt{M}\left\{[U_1 + (1-M)U_0]^2 + (1-M)U_2\right\}^{1/2}}{1-M}$$

and

$$\frac{U_1 - \sqrt{M}\left\{[U_1 + (1-M)U_0]^2 + (1-M)U_2\right\}^{1/2}}{1-M}.$$

Consecutive to the greedy search, tested $(M-3)$-tuples $\psi_2, \cdots, \psi_{M-2}$ may not exactly verify $F_1(\psi_2, \cdots, \psi_{M-2})$ or $F_2(\psi_2, \cdots, \psi_{M-2})$ equal to zero. We pick those $\psi_2, \cdots, \psi_{M-2}$ for which either $F_1(\psi_2, \cdots, \psi_{M-2})$ or $F_2(\psi_2, \cdots, \psi_{M-2})$ is below a predetermined threshold ε_1. This $(M-3)$-tuple $\psi_2, \cdots, \psi_{M-2}$ is completed by the properly computed ψ_{M-1}.

For each picked tuple $\psi_2, \cdots, \psi_{M-1}$, we compute $|T_2|/T_0$. The array is declared isotropic only if this ratio is below a predetermined threshold ε_2. We do so to discard situations where not only T_2, but also T_0 is close to zero.

The procedure ensures an antenna array with a minimal inter-sensor spacing lower than the specified distance d. It does not prevent the sensors from getting very close to each other, or even occupy the same position. After optimization, an ad-hoc test is conducted to discard such arrays.

During the exhaustive search, arrays that outperform the UCA are detected when the T_0 parameter is larger than that of the UCA (with the same inter-sensor spacing d), which can be easily shown to be equal to $Md^2/\left(4\sin^2(\pi/M)\right)$. A better-than-UCA array must, hence, verify

$$T_0 > \frac{Md^2}{4\sin^2(\pi/M)} \quad (5)$$

A computation search with a resolution of $2\pi/200$ is conducted with M equal to 4, 5, 6 and 7, respectively, and $d =$

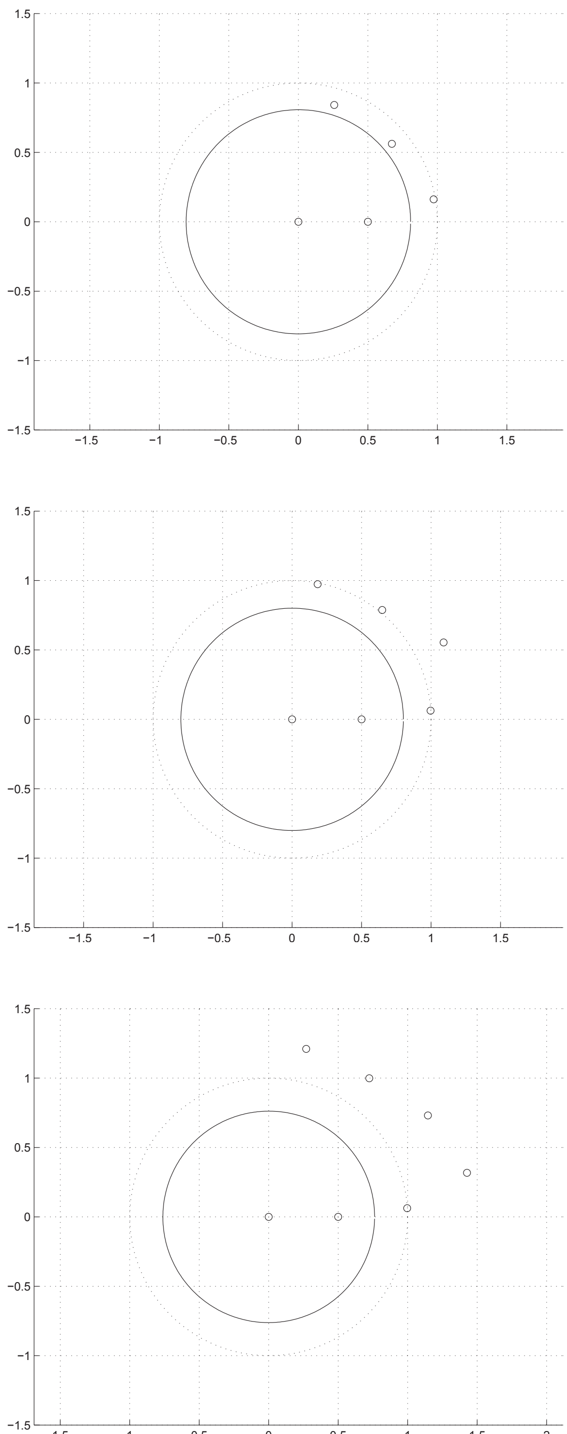

Fig. 3. Optimum 5, 6 and 7 sensors arrays.

$\lambda/2$. Parameters ε_1 and ε_2 are set to 0.01 and 0.001, respectively. It is shown that other-than-UCA array geometries exist that have an isotropic behavior. Their number increases dramatically as the number of sensors is incremented. To mention only the better-than-UCA arrays, we find that, except for the 4-sensors where the UCA is actually the best possible, numerous solutions verifying (5) are detected. The best ones (with the largest T_0) are plotted in Fig. 3, where, in addition to the sensor locations, we plot, in polar representation,

$$\frac{\mathcal{C}\left(\Phi\right)}{\mathcal{C}_{\mathrm{UCA}}\left(\Phi\right)} = \frac{M}{16\sin^2(\pi/M)T_0}$$

which is a circle contained in the unit circle. Fig. 3 suggest that the best isotropic array tends, as the number of sensors increases, to have a V shape. The achieved gain increases with M to reach 25%, for $M = 7$.

6. CONCLUSION

A CRB that takes into account the array ambiguity problem is developed. It yields to a condition on the sensor positions that ensures an isotropic behavior in DOA estimation. A systematic search is conducted to check this condition over the multi-dimensional space and, hence, identify all the possible isotropic ambiguity-free arrays. It leads to non-trivial conclusions. First, array geometries that do not have a circular symmetry may have an isotropic behavior. Second, the best over-all array geometry has a V shape and outperforms the UCA by 25%, in terms of DOA estimation MMSE.

7. REFERENCES

[1] H. Krim and M. Viberg, “Two decades of array signal processing research,” IEEE Signal Processing Mag., pp. 67-94, July 1996.

[2] B. Porat and B. Friedlander, “Analysis of the asymptotic relative efficiency of the MUSIC algorithm,” IEEE Trans. Acoust., Speech, Signal Processing, vol. 36, pp. 532-544, Apr. 1988.

[3] Y. Hua and T. K. Sarkar, “A note on the Cramer-Rao bound for 2-D direction finding based on 2-D array,” IEEE Trans. Signal Processing, vol. 39, pp. 1215-1218, May 1991.

[4] H. Gazzah and S. Marcos, “Cramer-Rao bounds for antenna array design,” IEEE Trans. Signal Processing, vol. 54, pp. 336-345, Jan. 2006.

[5] L. C. Godara and A. Cantoni, “Uniqueness and linear independence of steering vectors in array space,” J. Acoust. Soc. Am. 70(2), pp. 467-475, Aug. 1981.

[6] H. Gazzah and S. Marcos, “Analysis and design of (non-)isotropic arrays for 3D direction finding,” IEEE SSP’05 Conf., 17-20 July 2005, Bordeaux, France.